[3]C. S. Liu, M. N. Rosenbluth, and R. B. White, Phys. Fluids 17, 121 (1974); D. W. Forslund, J. M. Kindel, and E. L. Lindman, Phys. Fluids 18, 1002 (1975); W. Manheimer and H. Klein, Phys. Fluids 17, 1889 (1974); B. I. Cohen, A. N. Kaufman, and K. M. Watson, Phys. Rev. Lett. 29, 581 (1972); Kent Estabrook, D. Phillion, and V. Rupert, Lawrence Livermore Laboratory Laser Fusion Monthly Report, June 1979 (unpublished); W. L. Kruer, K. G. Estabrook, and K. H. Sinz, Nucl. Fusion 13, 952 (1973); J. J. Thomson, Phys. Fluids 21, 2082 (1978); T. Tajima and J. M. Dawson, Phys. Rev. Lett. 43, 267 (1979).

[4]J. F. Drake and Y. C. Lee, Phys. Rev. Lett. 31, 1197 (1973).

[5]W. L. Kruer, K. G. Estabrook, B. F. Lasinski, and A. B. Langdon, Phys. Fluids 23, 1326 (1980).

[6]D. W. Phillion, W. L. Kruer, and V. C. Rupert, Phys. Rev. Lett. 39, 1529 (1977).

[7]A. B. Langdon, B. F. Lasinski, and W. L. Kruer, Phys. Rev. Lett. 43, 133 (1979); A. B. Langdon and B. F. Lasinski, Phys. Rev. Lett. 34, 934 (1975); D. W. Forslund, J. M. Kindel, and K. Lee, to be published.

[8]M. N. Rosenbluth, Phys. Rev. Lett. 29, 565 (1972).

[9]M. Rosen *et al.*, Phys. Fluids 22, 2020 (1979), and private communication.

[10]D. Eimerl, private communication.

Observation of an Upper-Hybrid Soliton

Teruji Cho and Shigetoshi Tanaka
Department of Physics, Faculty of Science, Kyoto University, Kyoto 606, Japan
(Received 30 May 1980)

A density cavity at the upper-hybrid resonance layer has been observed in the saturated stage of the trapped electrostatic field when a high-power microwave of the extraordinary mode is injected into an afterglow plasma column in a uniform magnetic field. The results can be explained by the modulational instability at the upper-hybrid frequency and the formation of an upper-hybrid soliton.

PACS numbers: 52.35.Mw

In the absence of a magnetic field the density cavity near the electron plasma frequency ω_{pe} has been extensively studied.[1-4] In the presence of a magnetic field some aspects of the nonlinear modulation of the upper-hybrid wave have been examined theoretically.[5-8] Porkolab and Goldman[5] predicted that a high-power microwave forms an upper-hybrid envelope soliton. Such a phenomenon is worthy of study, since this effect may occur both in the electron cyclotron heating of toroidal plasmas[9-12] and also in laser-plasma interaction.[13] In this Letter we report the first experimental observation of a density cavity in the saturation stage of modulational instability at the upper-hybrid resonance (UHR) layer in a plasma column in a magnetic field.

The experiments were carried out in a linear machine. A vacuum vessel (11 cm in diameter, 125 cm in length) is located in a uniform magnetic field B (<3.5 kG). The pulsed dc discharge is produced at an argon gas pressure of $p=(5-10)\times 10^{-4}$ Torr by using an oxide cathode (3 cm in diameter). The experiments are performed in an afterglow plasma, whose typical parameters are an electron temperature $T_{e0}\approx 2.5$ eV and an electron density $n_{e0}\approx 2\times 10^{12}$ cm^{-3} at the center of the positive column. A high-power microwave ($\omega/2\pi = 9.4$ GHz, $P_\mu \leq 50$ kW and $\tau_\mu = 0.3-1.5$ μs) is injected into the plasma in the form of the extraordinary mode with use of a standard waveguide, whose end is located at $r=5.5$ cm from the center of the plasma column.

In Fig. 1(a) the radial profiles of the wave intensity I_μ and the electron density n_e are plotted when the low P_μ is injected from the left-hand side of the plasma column. The intensity I_μ is picked up by the probe located in front of the waveguide and sampled by a boxcar integrator. The incident microwave, passing the cyclotron cutoff, tunnels through the evanescent region and arrives at the UHR layer ($\omega=\omega_{UH}$), where it is converted to the electron Bernstein mode (EBM) which propagates towards the high-density region. This behavior is well known in the linear theory.[14-17] However, when a high P_μ is injected, an electron density depression (cavity, whose half-width is 3–4 mm,) is observed at the UHR layer [Fig. 1(b)]. The injected microwave seems to be trapped at the UHR layer, since the intensity I_μ at $\omega=\omega_{UH}$ increases drastically, while that of

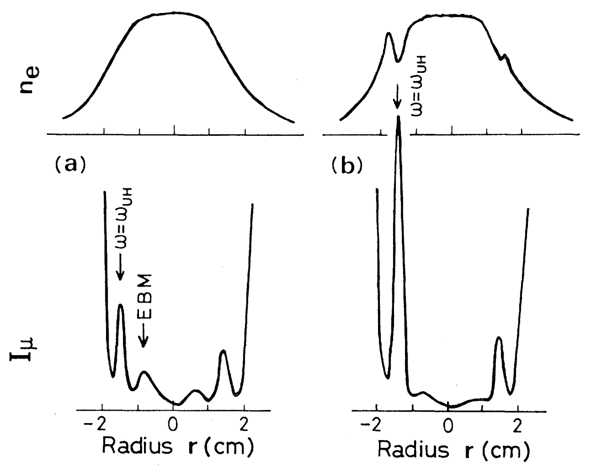

FIG. 1. Radial profiles of the wave intensity I_μ and the electron density n_e (electron saturation current I_e measured with a Langmuir probe). (a) Incident microwave power $P_\mu = 0.5$ kW, (b) 30 kW ($\tau_\mu = 350$ ns), respectively. The intensity I_μ is detected at $t = 200$ ns after P_μ is turned on, while the current I_e is sampled at $t = 150$ ns after P_μ is turned off. In (a) and (b) the microwave attenuators in the input and the detecting circuits are adjusted to receive the same level of I_μ in the absence of the plasma. $B = 0.6$ kG, $n_{e0} = 1.5 \times 10^{12}$ cm^{-3} and $p = 5\times 10^{-4}$ Torr.

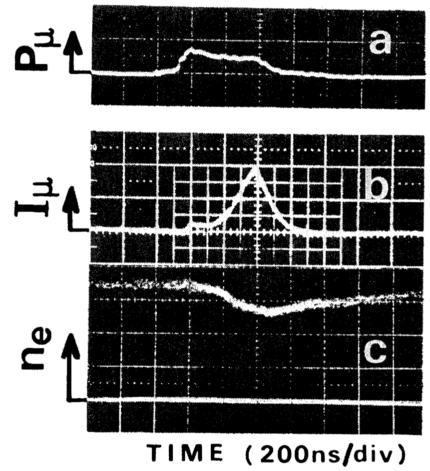

FIG. 2. The temporal evolutions of (b) the wave intensity I_μ and (c) the density depression at the UHR layer when (a) the high-power microwave $P_\mu = 25$ kW is applied.

EBM decreases, compared with the case of weak P_μ. The density cavity on the right of the plasma column is due to the microwave reflected from the right-hand side wall. Measurements of the axial profiles of $n_e(z)$ and $I_\mu(z)$ along the magnetic field at the radial position of the UHR layer show that the density cavity is about 25 mm in axial length and the half-width of $I_\mu(z)$ is from 25 to 30 mm, roughly equal to the long side width of the waveguide.

The temporal evolution of the instability of the wave intensity I_μ accompanying the density cavity is shown in Fig. 2. About 125 ns after the start of the injection of P_μ [Fig. 2(a)], the intensity I_μ at the UHR layer [Fig. 2(b)] begins to increase exponentially until I_μ is saturated at the peak of curve in Fig. 2(b). Corresponding to such an evolution of I_μ, the density depression Δn_e [Fig. 2(c)] appears with a depth $\Delta n_e/n_e$ reaching about 25%, and the depression lasts more than 1 μs.

As P_μ is increased, the delay time of the exponential growth of I_μ becomes short and the saturation value of the intensity, $I_{\mu\,\text{sat}}$, as well as the density depression Δn_e increases. Calibrating the absolute power of I_μ in Fig. 2(b), the temporal growth rate γ of I_μ is measured and plotted as a function of P_μ in Fig. 3(a). Here the ratio γ/ω is proportional to P_μ and becomes saturated when P_μ is very intense (> 30 kW). Both $I_{\mu\,\text{sat}}$ and $\Delta n_e/n_e$ increase and then become saturated as P_μ increases [Figs. 3(b) and 3(c)]. There is a threshold power $P_{\mu\,\text{thres}}$ (≈ 5 kW), above which the instability appears, and below $P_{\mu\,\text{thres}}$ the intensity I_μ is exactly proportional to P_μ with a small proportionality constant as shown by the straight section of I_μ for $P_\mu < P_{\mu\,\text{thres}}$.

We now compare the experimental results with the theoretical ones[5] for the upper-hybrid soliton with a small component of microwave field along the magnetic field. The nonlinear Schrödinger equation has been derived under the following conditions: The scale length, L_z, of the wave in the direction parallel to the field B is much larger than L_x, the scale length in the direction perpendicular to B, and γ is in the range $\Omega_i \ll \gamma \ll \Omega_e$. The wave should have positive dispersion ($\omega^2 \approx \omega_{\text{UH}}^2 + 3k^2 v_{Te}^2$) and n_e is high enough so that $\omega_{\text{UH}} \approx \omega_{pe} \gg \Omega_e$. Then the maximum γ of the modulational instability is given by[5]

$$\gamma = -\nu_e + \epsilon_0 \omega E_0^2/[8n_e(T_e + T_i)]. \quad (1)$$

Here ν_e is the electron collision frequency and E_0 is the pump field strength before the exponential growth. The above requirements are satisfied by our experiments with $\omega/\Omega_e = 5.7$, $\omega_{pe}/\Omega_e \approx 5.6$, $\Omega_i = 2.3 \times 10^6 \ll \gamma = 8.9 \times 10^6 \ll \Omega_e = 1.1 \times 10^{10}$ and L_z (≈ 25 mm) $\gg L_x$ (≈ 3–4 mm). It is noted that in the range of $P_\mu \lesssim 30$ kW the experimental value of γ/ω [Fig. 3(a)] is nearly proportional to P_μ ($\propto E_0^2$) as described by Eq. (1). Further, sub-

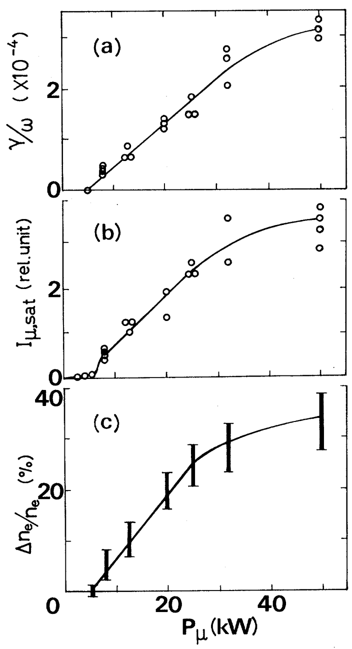

FIG. 3. (a) The growth rate γ of the wave intensity I_μ, (b) the saturated intensity $I_{\mu\ \mathrm{sat}}$ and (c) the depth of density cavity $\Delta n_e/n_e$ at the UHR layer are plotted as functions of the incident power P_μ.

stituting the experimental values ($\gamma/\omega = 1.5\times 10^{-4}$ for $P_\mu = 25$ kW and $\nu_e \approx 3$ MHz) into Eq. (1), we obtain $E_0 \approx 100$ V/cm, which is compatible with the experimentally estimated value of $E_0 \approx 150$ V/cm. This field grows exponentially and is saturated at a value 15–17 dB above the initial one; then the field pressure attains a value of $\epsilon_0 E^2/2n_e T_e \approx 0.1$. This should be compared with the experimental size of the depression, $\Delta n_e/n_e \approx 0.25$, since the theory[5] predicts that $\Delta n_e/n_e = \epsilon_0 E^2/2n_e T_e$. It is noted in Fig. 3(c) that the depression $\Delta n_e/n_e$ is proportional to the incident power $P_\mu\ (\propto E^2)$ as predicted theoretically and is saturated above $P_\mu = 30$ kW. In Figs. 3(a) and 3(b) there is a threshold of P_μ for the exponential growth of the wave. Substituting the experimental value of the threshold ($P_{\mu\ \mathrm{thres}} \approx 5$ kW) into Eq. (1), we obtain $\nu_e \approx 2$–3 MHz, which is compatible with $\nu_e = \nu_{ei} + \nu_{en} \approx 3$ MHz calculated from the collision frequency of electron with neutrals, $\nu_{en} \approx 2$ MHz at $p = 5\times 10^{-4}$ Torr, and that with ions, $\nu_{ei} \approx 1$ MHz at $T_e = 2.2$ eV and $n_e = 1\times 10^{12}$ cm^{-3}.

In the limit of $\nu_e = 0$, the solution of the upper-hybrid soliton is given by the usual hyperbolic secant.[5] Then if we assume that its slow time variation is proportional to γ, the half width of the soliton perpendicular to B is given by $L_x = (3\omega/\gamma)^{1/2} v_{Te}/\omega = 2\sqrt{6}(\omega_{pe}/\omega) T_e/eE_0$.[18] Experiments show that the measured half-width is nearly proportional to $P_\mu^{-1/2} \propto E_0^{-1}$.

The density cavity was observed at $\omega = \omega_{\mathrm{UH}}$ in the magnetic field range $\omega/\Omega_e = 2.8$–6.5, or, equiv-

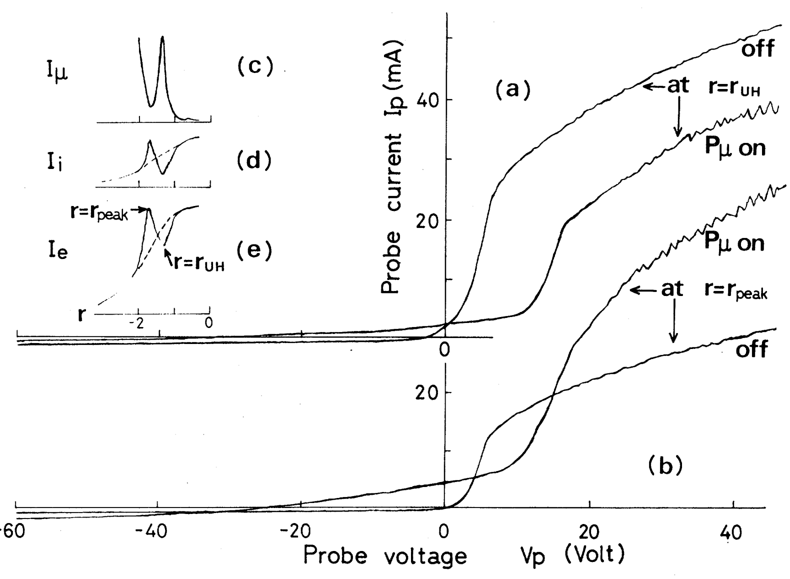

FIG. 4. Langmuir probe characteristics measured (a) at the UHR layer ($r = r_{\mathrm{UH}}$) and (b) at the low-density side of the cavity ($r = r_{\mathrm{peak}}$) in the presence and the absence of P_μ (25 kW, $\tau_\mu = 400$ ns). Radial profiles of (c) the wave intensity I_μ, (d) the ion saturation current I_i at $V_p = -52$ V and (e) the electron saturation current I_e at $V_p = 44$ V. These signals are sampled at $t = 350$ ns (gate, 50 ns) after P_μ being on.

alently, in the electron density range $\omega_{pe}/\Omega_e = 2.6-6.4$. It is notable that a strong depression ($\Delta n_e/n_e \simeq 0.35$ at $\omega/\Omega_e = 3.5$) was observed at $\omega/\Omega_e \approx s + 0.5$ ($s = 3,4,\ldots,6$) but the depression was weak at $\omega/\Omega_e = s$ ($\Delta n_e/n_e < 0.05$ at $\omega/\Omega_e = 3$). The results may correspond to the theoretical requirement that the condition for the soliton solution is fulfilled when the upper-hybrid wave has positive dispersion.[19] The theoretical prediction that no soliton should be formed in the low-density range of $\omega_{pe} < \Omega_e$ (or $\omega < \sqrt{2}\Omega_e$) could not be tested experimentally, since the afterglow plasma was so noisy in the strong field of $\omega < 2.8\Omega_e$ that a density cavity could not be ascertained distinctly.

It is remarkable that the upper-hybrid soliton accompanies suprathermal electrons. In Fig. 4(a) the background electron density is decreased, implying that a density cavity is formed, and an electron current appears even with a negative probe voltage when P_μ is injected. By analyzing the probe characteristics, we obtain suprathermal electrons having a temperature of $T_{supra} \approx 30$ eV and a density ratio to the background of $n_{supra}/n_e \approx 0.2$. As P_μ increases, n_{supra} and T_{supra} increase. It is noted that there is no temperature rise of background electrons during the pulse P_μ, which is seen from the exponentially rising sections of the curves, since by subtracting the contribution of the suprathermal electrons the slopes of the two curves (P_μ on and off) become the same. In the low-density side of the cavity ($r = r_{peak}$), the probe characteristics [curves in Fig. 4(b)] show that both the electron and ion densities increase to nearly double, and there appear suprathermals having $T_{supra} \approx 16$ eV and $n_{supra}/n_e \approx 0.25$. This density increase is shown in the radial profiles of I_i and I_e [curves in Figs. 4(d) and 4(e)]. However, such density increase and suprathermals could not be observed at the high-density side of the cavity. The production mechanism of these suprathermal electrons at $r = r_{UH}$ and r_{peak} is under study.

By injecting the microwave pulse P_μ, there is no temperature rise of the background electrons in $p = (5-10) \times 10^{-4}$ Torr, where the density cavity is observed. Here, the duration of the pulse ($\tau_\mu \approx 0.4$ μs) is too short to heat the electrons, since $\tau_\mu \approx \nu_e^{-1} \approx 0.4$ μs. In fact, electron heating due to upper-hybrid resonance occurs if τ_μ or p is increased. In the latter case ($p \approx 5 \times 10^{-3}$ Torr), we can observe a T_e rise to nearly double but cannot observe a density cavity. When p increases further ($p \gtrsim 7 \times 10^{-3}$ Torr), the ionization of neutrals is dominant and the electron density increases about 1.5 times; a density cavity cannot then be observed.

The results are summarized as follows: When the high power microwave is injected into the plasma, the wave intensity is enhanced strongly at the UHR layer, and its ponderomotive force leads to the formation of the density cavity, and also its strong field produces suprathermal electrons. These features can be interpreted on the basis of modulational instability at the upper-hybrid frequency and the formation of an envelope soliton.

[1]H. C. Kim, R. L. Stenzel, and A. Y. Wong, Phys. Rev. Lett. 30, 886 (1974).

[2]H. Ikezi, K. Nishikawa, and K. Mima, J. Phys. Soc. Jpn. 37, 766 (1974).

[3]A. Y. Wong and R. L. Stenzel, Phys. Rev. Lett. 34, 727 (1975).

[4]A. Hasegawa, *Plasma Instabilities and Nonlinear Effects* (Springer-Verlag, Berlin, 1975), p. 194.

[5]M. Porkolab and M. V. Goldman, Phys. Fluids 19, 872 (1976).

[6]A. N. Kaufman and L. Stenflo, Phys. Scr. 11, 269 (1975).

[7]M. Y. Yu and P. K. Shukla, Plasma Phys. 19, 889 (1977).

[8]J. G. Turner and T. J. M. Boyd, J. Plasma Phys. 22, 121 (1979).

[9]V. V. Alikaev *et al.*, Sov. J. Plasma Phys. 2, 212 (1976), and 3, 127 (1977) [Fiz. Plazmy 2, 390 (1976), and 3, 230 (1977)].

[10]R. M. Gilgenbach *et al.*, Phys. Rev. Lett. 44, 647 (1980).

[11]T. Cho *et al.*, Phys. Lett. 77A, 318 (1980), and to be published.

[12]T. Maekawa, S. Tanaka, Y. Terumichi, and Y. Hamada, Phys. Rev. Lett. 40, 1379 (1978); J. Phys. Soc. Jpn. 48, 247 (1980).

[13]Y. Kitagawa, Y. Yamada, I. Tsuda, M. Yokoyama, and C. Yamanaka, Phys. Rev. Lett. 43, 1875 (1979).

[14]K. Mitani, H. Kubo, and S. Tanaka, J. Phys. Soc. Jpn. 19, 211, 221 (1964).

[15]V. E. Golant and A. D. Piliya, Sov. Phys. Usp. 14, 413 (1972) [Usp. Fiz. Nauk 104, 413 (1971)].

[16]J. A. Tataronis and F. W. Crawford, J. Plasma Phys. 4, 231, 249 (1970).

[17]R. B. White and F. F. Chen. Plasma Phys. 16, 565 (1974).

[18]Since the soliton solution is given by $|E|^2 \propto \mathrm{sech}^2[(2\gamma/3\omega)^{1/2}(\omega/v_{Te})x]$ [Eq. (72) in Ref. 5], γ given by Eq. (1) is substituted.

[19]The electron Bernstein modes (Ref. 16) (with the positive dispersion branches forming the upper-hybrid wave) have a very weak positive dispersion at $\omega \gtrsim \omega_{UH}$ for $\omega_{UH} = s\Omega_e \pm \delta\Omega_e$ ($\delta << s$) and a negative dispersion at $\omega \lesssim s\Omega_e$ for $\omega_{UH} > s\Omega_e$.

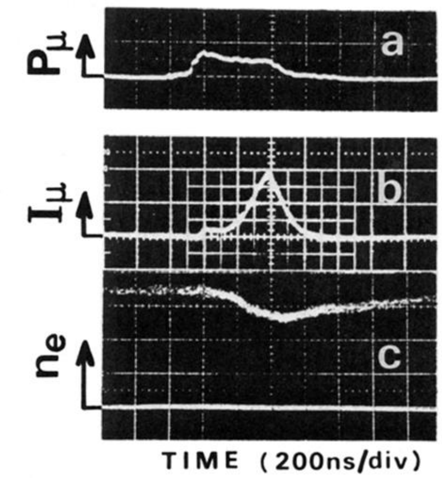

FIG. 2. The temporal evolutions of (b) the wave intensity I_μ and (c) the density depression at the UHR layer when (a) the high-power microwave P_μ = 25 kW is applied.